2017 IEEE 56th Annual Conference on Decision and Control (CDC)
December 12-15, 2017, Melbourne, Australia

Physics-Integrated Hierarchical/Distributed HVAC Optimization for Multiple Buildings with Robustness against Time Delays

Takeshi Hatanaka, Xuan Zhang, Wenbo Shi, Minghui Zhu and Na Li

Abstract— **In this paper, we address energy management for heating, ventilation, and air-conditioning (HVAC) systems in multiple buildings, and present a novel hierarchical/distributed optimization algorithm based on passivity. After formulating a thermal dynamics and an associated optimization problem across multiple buildings, we present a novel physics-integrated hierarchical/distributed optimization algorithm based on so-called primal-dual algorithm and the algorithm presented in [7]. We then prove convergence of the zone temperatures to the optimal ones based on passivity. The algorithm is further extended to ensure robustness against inter-layer time delays using scattering transformation. The present algorithm is finally demonstrated through simulation.**

I. Introduction

Buildings are one of sections consuming the largest energy, and reducing the consumption via smart energy management is expected to contribute to realizing sustainable society. In particular, motivated by the fact that about half of the consumed energy is occupied by heating, ventilation, and air-conditioning (HVAC) systems, a great deal of works have been devoted to HVAC optimization/control [1].

The most promising control methodology for HVAC optimization and control is Model Predictive Control (MPC) [1]–[6]. Indeed, several successful results have been reported in the literature. However, prediction of future state trajectories, inherent in MPC, requires state measurements and prediction of disturbances including the heat gain by the occupants. The state feedback may be problematic if temperatures of walls, floors, windows and ceilings are included as state variables. The heat gain prediction is discussed in [5], but the method and any learning techniques more or less have to presume that the heat follows the same pattern as the past data, which is not always true for some buildings.

In [7], the authors presented another solution requiring not prediction but current measurements of partial measurable states and disturbances, where the physical dynamics with a local controller is integrated with a set-point optimization process as an interconnection of dynamical systems.

This paper extends [7] to a more global problem to jointly optimize HVAC systems in multiple buildings. We first present the global optimization problem in the form of a resource allocation problem [9], where every building tries to solve a local problem in [7] while the total power consumption of all buildings is constrained by an upper bound. We then present a novel three-layer hierarchical/distributed control algorithm consisting of a power price update process, each building's local set-point optimization and local temperature controllers based on the primal-dual algorithm [8] and the algorithm in [7]. Stability and convergence of the resulting interconnected system are then proved based on passivity. We moreover extend the present algorithm to ensure robustness against communication delays between the price update process and the process of every building based on so-called scattering transformation [10]. Finally, the present algorithms are demonstrated through simulation.

The contribution of this paper is summarized as follows. To our knowledge, the present hierarchical/distributed control algorithm is itself novel, but related algorithms are found in the literature. If we ignore the physical dynamics, it is well known that the primal-dual algorithm provides a (two-layer) hierarchical/distributed architecture [9]. The contribution of this paper in this aspect is to integrate another layer, physical dynamics, while ensuring stability of the total system.

The architecture integrating physical dynamics and optimization dynamics is investigated in [11]–[16] mainly motivated by power grid optimization and control. In particular, the design concept presented in Section VII of [15] for power grid control is close to ours. However, the structural constraints on the optimization problem required therein are not satisfied in our problem. The approach of [11], [12] is specialized to power grid control and is not trivially applied to HVAC control. Meanwhile, Zhang et al. [16] address HVAC optimization for a single building and interconnect physical dynamics with the primal-dual algorithm. However, the algorithm requires measurements of states and their derivatives, which are not always acquired in practice. The same statement is also applied to [14]. Passivity-based HVAC control design is addressed in [17], but interconnections with optimization are not discussed therein.

Finally, time delays are investigated in none of the above works. Leaving the physical dynamics aside, time delays in distributed optimization are investigated in [18], [20], [19]. However, [18], [20] do not ensure exact convergence to an optimal solution, whereas we do. The problem formulation investigated in [19] is different from this paper. Thus, this paper also adds a contribution to the field of distributed optimization.

II. Problem Settings

In this paper, we consider multiple buildings $b = 1, 2, \ldots, N$, where each building b consists of multiple zones $i = 1, 2, \ldots, n^b$. Suppose that the zones $i =$

T. Hatanaka is with School of Engineering, TokyoTech, Tokyo 152-8552, JAPAN. hatanaka@ctrl.titech.ac.jp. X. Zhang, W. Shi and N. Li are with Electrical Engineering and Applied Mathematics of the School of Engineering and Applied Sciences, Harvard Univ., 33 Oxford St, Cambridge, MA 02138, USA. M. Zhu is with Department of Electrical Engineering, Pennsylvania State Univ., University Park, PA 16802, USA.

978-1-5090-2872-6/17/$31.00 ©2017 IEEE

$1,2,\ldots,n_1^b$ ($n_1^b \le n^b$) are equipped with VAV (Variable Air Volume) HVAC systems while $i = n_1^b+1,\ldots,n^b$ ($n_2^b := n^b - n_1^b$) do not have (active) HVAC systems, which may include walls, windows, corridors and rooms not in use.

In the sequel, we take the following notations. The temperature, mass flow rate, heat gain from external sources like occupants of zone i in building b are respectively denoted by T_i^b, m_i^b and q_i^b. Denote also the ambient temperature by $T^{\rm a}$. The thermal capacitance, thermal resistance of zone i in building b are denoted by C_i^b and R_i^b respectively and the thermal resistance between zone i and j is denoted by R_{ij}^b. The temperature of the air supplied to zone i in building b is denoted by $T_i^{\rm sb}$ and the specific heat is denoted by a_i^b.

A. System Description

In this subsection, we briefly review the thermal dynamics of each building presented in [7]. See Section II-B of [7] for more details on the model.

The thermal dynamics of every building b is assumed to be modeled by the RC circuit model

$$C^b\dot{T}^b = R^bT^{\rm a}\mathbf{1} - (R^b+L^b)T^b + B^bG^b(T^b)m^b + B^bq^b,$$

where T^b, q^b and m^b are collections of T_i^b ($i=1,2,\ldots,n^b$), q_i^b ($i=1,2,\ldots,n_1^b$), and m_i^b ($i=1,2,\ldots,n_1^b$) respectively. The matrices C^b and R^b are diagonal matrices with diagonal elements C_i^b ($i=1,2,\ldots,n^b$) and $\frac{1}{R_i^b}$ ($i=1,2,\ldots,n^b$), respectively. The matrix L^b describes the weighted graph Laplacian with elements $\frac{1}{R_{ij}^b}$, $G^b(T^b) \in \mathbb{R}^{n_1^b\times n_1^b}$ is a block diagonal matrix with diagonal elements equal to $a_i^b(T_i^{\rm sb} - T_i^b)$ ($i=1,2,\ldots,n_1^b$), $\mathbf{1}$ is the real vector whose elements are all 1, and $B^b = [I_{n_1^b}\ 0]^\top \in \mathbb{R}^{n^b\times n_1^b}$.

We next linearize the model at around an equilibrium, and transform the variables as

$$\begin{aligned} x^b &:= (C^b)^{1/2}\delta T^b,\ u^b := (B^b)^\top (C^b)^{-1/2}B^bG^b(\bar{T}^b)\delta m^b,\\ w_{\rm a}^b &:= (C^b)^{-1/2}R^b\delta T^{\rm a}\mathbf{1},\ w_{\rm q}^b := (B^b)^\top(C^b)^{-1/2}B^b\delta q^b \end{aligned} \tag{1}$$

where δT^b, δm^b, $\delta T^{\rm a}$ and δq^b describe the errors between T^b, m^b, $T^{\rm a}$ and q^b and the corresponding equilibrium states and inputs respectively, and $\bar{T}^b$ is the collection of temperatures at the selected equilibrium. The resulting model then takes the form of

$$\dot{x}^b = -A^bx^b + B^bu^b + B^bw_{\rm q}^b + w_{\rm a}^b,\ x^b := \begin{bmatrix} x_1^b\\ x_2^b\end{bmatrix}, \tag{2}$$

where $x^b \in \mathbb{R}^{n^b}$, $u^b \in \mathbb{R}^{n_1^b}$ $w_{\rm q}^b \in \mathbb{R}^{n_1^b}$, $w_{\rm a}^b \in \mathbb{R}^{n^b}$, $x_1^b \in \mathbb{R}^{n_1^b}$, $x_2^b \in \mathbb{R}^{n_2^b}$, and A^b is positive definite [7].

We assume that the measured outputs are restricted to x_1^b and $w_{\rm a}^b$, and that the heat gain $w_{\rm q}^b$ is not measurable.

B. Optimization Problem

Let us now consider the following optimization problem.

$$\min_{z^1,\ldots,z^N} \sum_{b=1}^N \{\frac{1}{2}\|z_{x1}^b - h^b\|^2 + f^b(z_u^b)\} \tag{3a}$$

$$\text{subject to: } g^b(z_u^b) \le 0,\ b=1,2,\ldots,N \tag{3b}$$

$$-A^bz_x^b + B^bz_u^b + B^bd_{\rm q}^b + d_{\rm a}^b = 0,\ b=1,2,\ldots,N \tag{3c}$$

$$g^0(z_u^1,\ldots,z_u^N) := \sum_{b=1}^N \bar{f}^b(z_u^b) - \gamma \le 0 \tag{3d}$$

with

$$z^b := \begin{bmatrix} z_x^b\\ z_u^b\end{bmatrix},\ z_x^b := \begin{bmatrix} z_{x1}^b\\ z_{x2}^b\end{bmatrix},\quad \begin{matrix} z_x^b \in \mathbb{R}^{n^b},\ z_u^b \in \mathbb{R}^{n_1^b}\\ z_{x1}^b \in \mathbb{R}^{n_1^b},\ z_{x2}^b \in \mathbb{R}^{n_2^b}\end{matrix}.$$

The variables z_x^b and z_u^b correspond to the zone temperature x^b and mass flow rate u^b after the transformation (1), respectively. The parameters $d_{\rm q}^b \in \mathbb{R}^{n_1^b}$ and $d_{\rm a}^b \in \mathbb{R}^{n^b}$ represent DC components of the disturbances $w_{\rm q}^b$ and $w_{\rm a}^b$, respectively. The equality constraint (3c) corresponds to the stationary equation of the dynamics (2).

The first term of the cost (3a) evaluates the human comfort, where $h^b \in \mathbb{R}^{n_1^b}$ is the collection of the most comfortable temperatures for occupants in zones $i = 1,2,\ldots,n_1^b$. The function $f^b : \mathbb{R}^{n_1^b} \to \mathbb{R}$ is a cost function for reducing the power consumption. The constraint function $g^b : \mathbb{R}^{n_1^b} \to \mathbb{R}^{c^b}$ reflects hardware constraints on the mass flow rate and/or an upper bound of the power consumption. The inequality (3d) is a global constraint across all buildings to bound the total power consumption for $b=1,2,\ldots,N$, where $\bar{f}^b$ provides the power consumption of building b.

Assumption 1 (i) The function f^b and $\bar{f}^b$ are convex, differentiable and their gradients are locally Lipschitz for all $b = 1,2,\ldots,N$, (ii) every element of the function g^b is convex, differentiable and its gradient is locally Lipschitz for all $b = 1,2,\ldots,N$, (iii) there exists z_u^b ($b=1,2,\ldots,N$) such that $g^b(z_u^b) < 0$ for all $b=1,2,\ldots,N$ and $g^0(z_u^1,\ldots,z_u^N) < 0$.

See Section II-C of [7] for the detailed discussions on validity of the formulation (3) and the assumption.

We next eliminate the variable z_x^b from (3) using (3c) as

$$\min_{z_u^1,\ldots,z_u^N} \sum_{b=1}^N \{\phi^b(z_u^b) + f^b(z_u^b)\} \tag{4a}$$

$$\text{subject to: } g^b(z_u^b) \le 0,\ b=1,2,\ldots,N \tag{4b}$$

$$g^0(z_u^1,\ldots,z_u^N) := \sum_{b=1}^N \bar{f}^b(z_u^b) - \gamma \le 0 \tag{4c}$$

$$\phi^b(z_u^b) := \frac{1}{2}\|M^b(z_u^b + d_{\rm q}^b) + (B^b)^\top(A^b)^{-1}(d_{\rm a}^b - \bar{h}^b)\|^2$$

where $M^b := (B^b)^\top(A^b)^{-1}B^b$ and $\bar{h}^b := A^bB^bh^b$. Note that since A^b is positive definite, M^b is also positive definite, which means that the function ϕ^b is strongly convex in z_u^b. Then, there exists a unique solution to (4), denoted by $z_u^{b*} \in \mathbb{R}^{n_1^b}$ ($b=1,2,\ldots,N$), which must satisfy the following

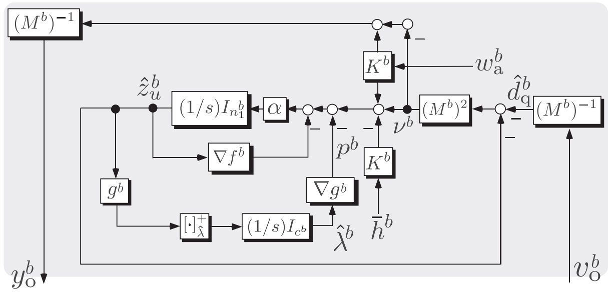

Fig. 1. Block diagram of optimization dynamics (11).

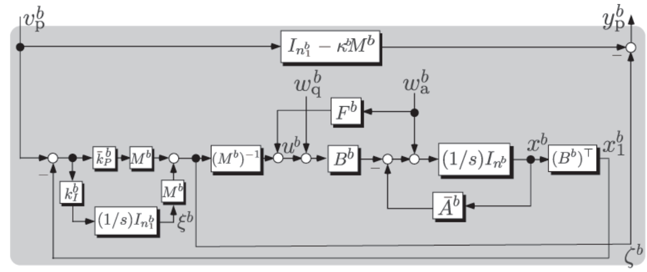

Fig. 2. Block diagram of physical dynamics (2) with controller (12).

KKT condition [9], where $K^b := M^b(B^b)^\top(A^b)^{-1}$, and $\circ$ represents the Hadamard product.

$$(M^b)^2(z_u^{b*} + d_{\rm q}^b) + K^b(d_{\rm a}^b - \bar{h}^b) + \nabla f^b(z_u^{b*}) \\ + \nabla g^b(z_u^{b*})\lambda^{b*} + \nabla \bar{f}^b(z_u^{b*})\lambda^{0*} = 0 \ \ \forall b \tag{5a}$$

$$g^b(z_u^{b*}) \le 0, \ \lambda^{b*} \ge 0, \ \lambda \circ g^b(z_u^{b*}) = 0 \ \ \forall b \tag{5b}$$

$$g^0(z_u^{1*}, \ldots, z_u^{N*}) \le 0, \lambda^{0*} \ge 0, g^0(z_u^{1*}, \ldots, z_u^{N*})\lambda^{0*} = 0 \tag{5c}$$

Since (4) is essentially equivalent to (3), if we define

$$z_x^{b*} := (A^b)^{-1}(B^b z_u^{b*} + B^b d_{\rm q}^b + d_{\rm a}^b) \in \mathbb{R}^{n^b}, \tag{6}$$

the collection of $z^{b*} := [(z_x^{b*})^\top \ (z_u^{b*})^\top]^\top$ for all $b = 1, 2, \ldots, N$ is a solution to (3). Divide z_x^{b*} as $z_x^{b*} := [(z_{x1}^{b*})^\top \ (z_{x2}^{b*})^\top]^\top$ ($z_{x1}^{b*} \in \mathbb{R}^{n_1^b}$, $z_{x2}^{b*} \in \mathbb{R}^{n_2^b}$). We then have

$$z_{x1}^{b*} = M^b(z_u^{b*} + d_{\rm q}^b) + (B^b)^\top(A^b)^{-1}d_{\rm a}^b \in \mathbb{R}^{n_1^b}. \tag{7}$$

The objective of this paper is to design a controller so as to ensure convergence of the actual room temperature x_1^b to the optimal room temperature z_{x1}^{b*}, the solution to (4), without direct measurements of $w_{\rm q}^b$ for all $b = 1, 2, \ldots, N$.

III. Physics-Integrated Hierarchical/Distributed Optimization Algorithm

The problem (4) belongs to a class of so-called resource allocation problems with separable constraints and costs [9]. A distributed solution to this kind of problem is known to be given by the primal-dual gradient algorithm [8]:

$$\dot{\hat{z}}_u^b = -\alpha\{(M^b)^2(\hat{z}_u^b + d_{\rm q}^b) + K^b(d_{\rm a}^b - \bar{h}^b) + \nabla f^b(\hat{z}_u^b) \\ + \nabla g^b(\hat{z}_u^b)\hat{\lambda}^b + p_b^0\}, \ b = 1, 2, \ldots, N, \tag{8a}$$

$$\dot{\hat{\lambda}}^b = [g^b(\hat{z}_u^b)]^+_{\hat{\lambda}^b}, \ b = 1, 2, \ldots, N, \tag{8b}$$

$$\dot{\hat{\lambda}}^0 = [g^0(\hat{z}_u^1, \ldots, \hat{z}_u^N)]^+_{\hat{\lambda}^0}, \ p^0 = \nabla g^0(\hat{z}_u^1, \ldots, \hat{z}_u^N)\hat{\lambda}^0, \tag{8c}$$

where $\hat{z}_u^b \in \mathbb{R}^{n_1^b}$, $\hat{\lambda}^b \in \mathbb{R}^{c^b}$ and $\hat{\lambda}^0 \in \mathbb{R}$ are estimates of z_u^{b*}, λ^{b*} and λ^{0*}, respectively, $\alpha > 0$ and $p^0 = [(p_1^0)^\top \ \cdots \ (p_N^0)^\top]^\top$ ($p_b^0 \in \mathbb{R}^{n_1^b}$). The notation $[g]^+_\lambda$ for real vectors g, λ with the same dimension provides a vector whose l-th element, denoted by $([g]^+_\lambda)_l$, is given by

$$([g]^+_\lambda)_l = \begin{cases} 0, & \text{if } \lambda_l = 0 \text{ and } g_l < 0 \\ g_l, & \text{otherwise} \end{cases}, \tag{9}$$

where g_l, λ_l are the l-th elements of g, λ, respectively.

Given $d_{\rm q}^b$ and $d_{\rm a}^b$ for all $b = 1, 2, \ldots, N$, the variable $\hat{z}_u^b$ generated by the algorithm (8) converges to the optimal solution z_u^{b*} [8]. However, in practice, it is desired that $d_{\rm q}^b$ and $d_{\rm a}^b$ are updated in real time according to the changes of disturbances. It is now to be noted that $d_{\rm q}^b$ is not directly obtained since $w_{\rm q}^b$ is not measurable. We thus need to estimate $d_{\rm q}^b$ from the measurements of physical quantities, which motivates us to interconnect the physical dynamics (2) with the optimization dynamics (8).

The above problem for a single building is investigated in [7], and here we take the same architecture. The details on the background of the architecture are left to [7], but the basic concept is as follows: (i) estimated optimal zone temperatures generated by the optimization dynamics are sent to the physical dynamics as reference signals, and (ii) design a controller so that x_1^b tracks the reference, and an estimate of $Md_{\rm q}^b$ generated by the controller is sent back to the optimization dynamics.

We first replace $d_{\rm q}^b$ and $d_{\rm a}^b$ in (8a) by an estimate $\hat{d}_{\rm q}^b$ and the measurement $w_{\rm a}^b$ respectively, which yields

$$\dot{\hat{z}}_u^b = -\alpha\{(M^b)^2(\hat{z}_u^b + \hat{d}_{\rm q}^b) + K^b(w_{\rm a}^b - \bar{h}^b) \\ + \nabla f^b(\hat{z}_u^b) + \nabla g^b(\hat{z}_u^b)\hat{\lambda}^b + p_b^0\}. \tag{10}$$

The estimate $\hat{d}_{\rm q}^b$ is then regarded as an external input to the system (10). We next define an output signal $y_{\rm o}^b := M^b(\hat{z}_u + \hat{d}_{\rm q}^b) + (B^b)^\top(A^b)^{-1}w_{\rm a}^b$, and transform the input $\hat{d}_{\rm q}^b$ as $v_{\rm o}^b := M^b\hat{d}_{\rm q}^b$, which is needed to ensure passivity of the system [7]. The system (10) and (8b) is then reformulated as

$$\dot{\hat{z}}_u^b = -\alpha\{(M^b)^2\hat{z}_u^b + M^b v_{\rm o}^b + K^b(w_{\rm a}^b - \bar{h}^b) \\ + \nabla f^b(\hat{z}_u^b) + \nabla g^b(\hat{z}_u^b)\hat{\lambda}^b + p_b^0\}, \tag{11a}$$

$$\dot{\hat{\lambda}}^b = [g^b(\hat{z}_u^b)]^+_{\hat{\lambda}^b}, \tag{11b}$$

$$y_{\rm o}^b = M^b\hat{z}_u + v_{\rm o}^b + (B^b)^\top(A^b)^{-1}w_{\rm a}^b. \tag{11c}$$

Remark that, from (7), $y_{\rm o}^b$ is regarded as an estimate of the optimal zone temperatures z_{x1}^{b*}. The block diagram of the system is illustrated in Fig. 1.

Let us next consider the physical dynamics (2), and design the following controller to let x_1^b track a reference $v_{\rm p}^b$.

$$\dot{\xi}^b = k_{\rm I}^b(v_{\rm p}^b - x_1^b) \tag{12a}$$

$$u^b = k_{\rm P}^b(v_{\rm p}^b - x_1^b) + \xi^b + \kappa^b v_{\rm p}^b + F^b w_{\rm a}^b \tag{12b}$$

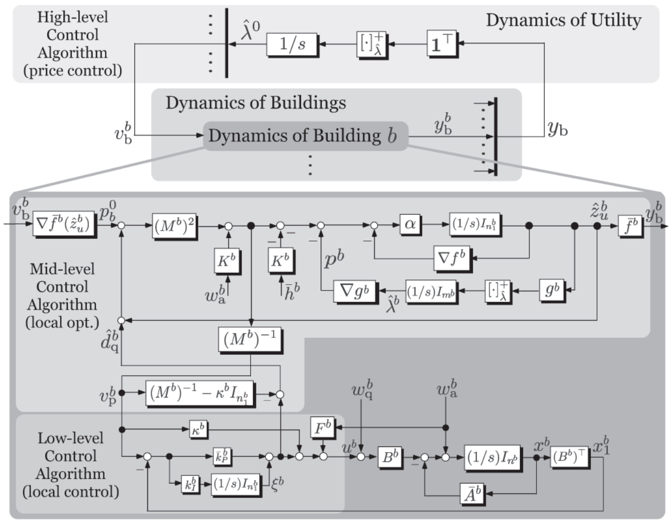

Fig. 3. Block diagram of the three layer control algorithm.

where $k_{\rm P}^b,\ k_{\rm I}^b,\ \kappa^b > 0,\ F^b := [-I_{n_1^b}\ (A_2^b)^\top (A_3^b)^{-1}]$[1]. Substituting (12) into (2) yields

$$\dot{x}^b = -A^b x^b + k_{\rm P}^b B^b (v_{\rm p}^b - x_1^b) + B^b \xi^b + \kappa^b B^b v_{\rm p}^b + B^b w_{\rm q}^b + (B^b F^b + I_{n^b}) w_{\rm a}^b, \quad (13a)$$

$$\dot{\xi}^b = k_{\rm I}^b (v_{\rm p}^b - x_1^b). \quad (13b)$$

We then define the output signal of (13) as

$$y_{\rm p}^b = \{(k_{\rm P}^b + 2\kappa^b) M^b - I_{n_1^b}\} v_{\rm p}^b - (k_{\rm P}^b + \kappa^b) M^b x_1^b + M^b \xi^b. \quad (14)$$

Here, we skip the details but this signal is regarded as an estimate of $-M^b d_{\rm q}^b$ (See Section V of [7]). The block diagram of the physical dynamics (13) is shown in Fig. 2.

We then interconnect (11) and (13) via negative feedback

$$v_{\rm o}^b = -y_{\rm p}^b,\ v_{\rm p}^b = y_{\rm o}^b. \quad (15)$$

Stability and convergence for (11), (13)–(15) with $\hat{p}^0 = 0$ are proved in Theorem 1 of [7], while convergence of (8) for given $d_{\rm q}^b$ and $d_{\rm a}^b$ is presented in [8]. However, properties of the interconnected system (8c), and (11), (13)–(15) are still unclear, which will be analyzed in the next section.

In the remainder of this section, we discuss implementation of the present algorithm. Notice now that the variable $\hat{\lambda}^0$ is known to be regarded as a price of the power [9]. We assume that the price is updated by a subject other than the buildings, and the subject is called utility in this paper.

Let us now equivalently transform the system (11), (13)–(15) into Fig. 3. The top block, Dynamics of Utility, describes the process to be executed by the utility. This figure means that the utility just collects and summarizes the estimated power consumptions $\bar{f}^b(\hat{z}_u^b)$, determined in the lower layers in real time, and updates the price $\hat{\lambda}^0$ according to

$$\dot{\hat{\lambda}}^0 = [\mathbf{1}^\top v_{\rm u} - \gamma]_{\hat{\lambda}^0}^+, \quad y_{\rm u} := [y_{\rm u}^1\ \cdots\ y_{\rm u}^N]^\top = \mathbf{1}\hat{\lambda}^0, \quad (16)$$

where $v_{\rm u} = y_{\rm b} := [y_{\rm b}^1\ \cdots\ y_{\rm b}^N]^\top \in \mathbb{R}^N$ and $y_{\rm b}^b := \bar{f}^b(\hat{z}_u^b)$. The utility then sends back $y_{\rm u}^b = \hat{\lambda}^0$ to each building b as the signal $v_{\rm b}^b$. Differently from (8c), (16) requires neither the local variables $\hat{z}_u^b$, nor knowledge on the local functions $\bar{f}^b$.

Let us next consider the process executed in each building, which is essentially equivalent to the interconnection of Figs. 1 and 2 via (15), but the input-output variables are slightly modified. The low-level control algorithm determines the mass flow rate u^b based on the reference $v_{\rm p}^b$ received from the middle-level algorithm and sends back the disturbance estimate $\hat{d}_{\rm q}^b$. The modification of the input-output variables ensures that the low-level controller is decentralized in the level of zones $i = 1, 2, \ldots, n_1^b$, which allows one to implement (12) at each zone similarly to the existing systems.

The middle-level algorithm receives the power price $v_{\rm b}^b = y_{\rm u}^b = \hat{\lambda}^0$ from the high-level algorithm and the disturbance estimate $\hat{d}_{\rm q}^b$ from the low-level one. It first computes $p_b^0 = \nabla \bar{f}^b(\hat{z}_u^b) v_{\rm b}^b$. The variable $\hat{z}_u^b$ is then updated according to (10), and the estimated power consumption $\bar{f}^b(\hat{z}_u^b)$ is sent back to the high-level and the estimated optimal temperature $y_{\rm o}^b$ is back to the low-level as the reference $v_{\rm p}^b$. These processes do not require any local variables and local costs and constrains of the other buildings, namely the algorithm is distributed in the level of buildings.

IV. Passivity, Convergence and Stability

In this section, we analyze convergence and stability of the present system. We first focus on the process of building b, which is equivalently transformed into Fig. 4. The system colored by light gray is formulated as

$$\dot{\hat{z}}_u^b = \alpha\{\mu^b + K^b \bar{h}^b - \nabla f^b(\hat{z}_u^b) - \nabla g^b(\hat{z}_u^b)\hat{\lambda}^b\}, \quad (17a)$$

$$\dot{\hat{\lambda}}^b = [g^b(\hat{z}_u)]_{\hat{\lambda}^b}^+, \quad (17b)$$

with input μ^b and output $\hat{z}_u^b$. The dark gray is given as

$$\dot{x}^b = -A^b x^b + k_{\rm P}^b B^b (v_{\rm p}^b - x_1^b) + \kappa^b B^b v_{\rm p}^b + B^b \xi^b + B^b w_{\rm q}^b + (B^b F^b + I_{n^b}) w_{\rm a}^b, \quad (18a)$$

$$\dot{\xi}^b = k_{\rm I}^b (v_{\rm p}^b - x_1^b), \quad (18b)$$

$$\zeta^b = (k_{\rm P}^b + \kappa^b) M^b (v_{\rm p}^b - x_1^b) + M^b \xi^b, \quad (18c)$$

whose input is $v_{\rm p}^b$ and output is ζ^b. The middle gray system is the collection of static equations which are simplified to

$$\zeta^b = -\kappa^b \nu^b + M^b \hat{z}_u^b + (B^b)^\top (A^b)^{-1} w_{\rm a}^b, \quad (19a)$$

$$\nu^b = M^b v_{\rm p}^b. \quad (19b)$$

Following the same procedure as Lemmas 6 and 7 in [7], we can immediately prove the following lemma.

Lemma 1 Suppose $w_{\rm a}^b \equiv d_{\rm a}^b$. Then, under Assumption 1, the system (17) with $\hat{\lambda}^b(0) \geq 0$ is passive from $\tilde{\mu}^b := \mu^b - \mu^{b*}$ to $\tilde{z}_u^b := \hat{z}_u^b - z_u^{b*}$ for all $b = 1, 2, \ldots, N$, where

$$\mu^{b*} := -(M^b)^2 (z_u^{b*} + d_{\rm q}^b) - K^b d_{\rm a}^b - \nabla \bar{f}^b(z_u^{b*})\lambda^{0*}. \quad (20)$$

[1] The matrices A_2^b and A_3^b are subblocks of A^b defined as

$$A^b = \begin{bmatrix} A_1^b & (A_2^b)^\top \\ A_2^b & A_3^b \end{bmatrix},\ A_1^b \in \mathbb{R}^{n_1^b \times n_1^b},\ A_3^b \in \mathbb{R}^{n_2^b \times n_2^b}.$$

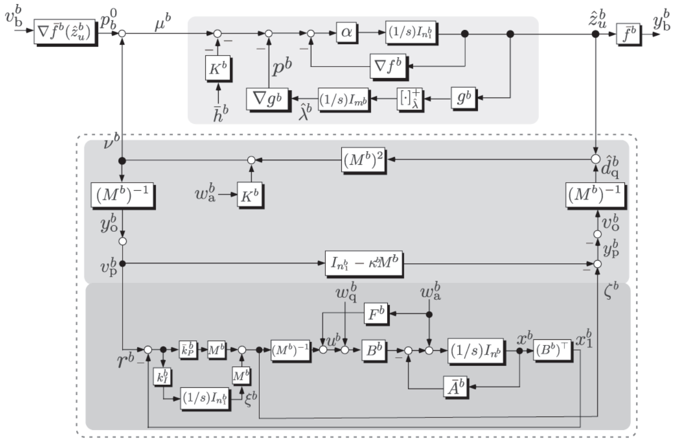

Fig. 4. Block diagram of building dynamics as feedback interconnection of passive systems, where the light gray system is passive (Lemma 1), and the system enclosed by the dotted line is passive (Lemma 2).

Let us now add the following assumption, which is expected to be true in most of the buildings since the diagonal elements tend to be dominant both for A_1^b and M^b [7].

Assumption 2 The matrix $M^bA_1^b + A_1^bM^b$ is positive definite for all $b = 1, 2, \ldots, N$.

Then, κ^b is assumed to be selected so that

$$M^bA_1^b + A_1^bM^b - 2\kappa^bM^b > 0. \tag{21}$$

We then have the following lemma on the system interconnecting (18) and (19).

Lemma 2 Suppose $w_{\rm a}^b \equiv d_{\rm a}^b$ and $w_{\rm q}^b \equiv d_{\rm q}^b$. Then, under Assumption 2, the system (18) and (19) is passive from $\tilde{z}_u^b$ to $\tilde{\nu}^b := \hat{\nu}^b - \nu^{b*}$ for all $b = 1, 2, \ldots, N$, where

$$\nu^{b*} := M^b z_{x1}^{b*} = (M^b)^2(z_u^{b*} + d_{\rm q}^b) + K^b d_{\rm a}^b. \tag{22}$$

The original system (11), (13)–(15) is given by interconnecting the system (17) and system (18), (19) via

$$\mu^b = -p_b^0 - \nu^b. \tag{23}$$

Lemmas 1 and 2 now provide an insight not presented in [7] that the system is a feedback interconnection of passive systems. This perspective and the well-known passivity preservation w.r.t. the feedback interconnection [10], [21] lead us to the following result.

Lemma 3 Suppose $w_{\rm a}^b \equiv d_{\rm a}^b$ and $w_{\rm q}^b \equiv d_{\rm q}^b$. Then, under Assumptions 1 and 2, the system (17)–(19) and (23) with $\hat{\lambda}^b(0) \geq 0$ is passive from $-\tilde{p}_b^0$ to $\tilde{z}_u^b$ for all $b = 1, 2, \ldots, N$, where $p_b^0 := p_b^0 - p_b^{0*}$ and $p_b^{0*} := \nabla \bar{f}^b(z_u^{b*})\lambda^{0*}$.

Following Fig. 4, we transform the system input from p_b^0 to $v_{\rm b}^b$ so that $p_b^0 = (\nabla \bar{f}^b(\hat{z}_u^b))v_{\rm b}^b$ and output from $\hat{z}_u^b$ to $y_{\rm b}^b := \bar{f}^b(\hat{z}_u^b)$. Passivity is then shown to be preserved as follows.

Lemma 4 Under the same assumptions as Lemma 3 and $v_{\rm b}^b \geq 0$ for all time, the system in Lemma 3 is passive from $-\tilde{v}_{\rm b}^b$ to $\tilde{y}_{\rm b}^b := y_{\rm b}^b - y_{\rm b}^{b*}$ for all b, where $\tilde{v}_{\rm b}^b := v_{\rm b}^b - v_{\rm b}^{b*}$ and

$$v_{\rm b}^{b*} := \lambda^{0*},\ y_{\rm b}^{b*} := \bar{f}^b(z_u^{b*}). \tag{24}$$

Noticing that (17)–(19) with (23) for each b is independent of other buildings, Lemma 4 immediately means that the collection of the systems for all b is passive from the collection of inputs $\tilde{v}_{\rm b} := [(\tilde{v}_{\rm b}^1)^\top\ \cdots\ (\tilde{v}_{\rm b}^N)^\top]^\top$ to the collection of outputs $\tilde{y}_{\rm b} := [(\tilde{y}_{\rm b}^1)^\top\ \cdots\ (\tilde{y}_{\rm b}^N)^\top]^\top$.

We next focus on the utility dynamics (16). Then, the same procedure as Lemma 1 of [7] proves the following result.

Lemma 5 Consider the system (16) with $\hat{\lambda}^0(0) \geq 0$. Then, under Assumption 1, it is passive from $\tilde{v}_{\rm u} := v_{\rm u} - v_{\rm u}^*$ to $\tilde{y}_{\rm u} := y_{\rm u} - y_{\rm u}^*$ with respect to the storage function $S^0 := \frac{1}{2}\|\hat{\lambda}^0 - \lambda^{0*}\|^2$, where

$$v_{\rm u}^* := [\bar{f}^1(z_u^{1*})\ \cdots\ \bar{f}^N(z_u^{N*})]^\top,\ y_{\rm u}^* := \lambda^{0*}\mathbf{1}. \tag{25}$$

More precisely, the following inequality is shown to hold.

$$D^+S^0 \leq \tilde{y}_{\rm u}^\top \tilde{v}_{\rm u}, \tag{26}$$

where D^+ describes the upper Dini derivative.

The entire system consists of the utility dynamics (16) and collection of the building dynamics (17)–(19) with (23) for all $b = 1, 2, \ldots, N$ via $v_{\rm u} = y_{\rm b}$ and $v_{\rm b} = y_{\rm u}$. In this case, $v_{\rm b}^b = \hat{\lambda}^0\mathbf{1}$ satisfies $v_{\rm b}^b \geq 0$ assumed in Lemma 4, which is confirmed from (16). Lemmas 4 and 5 thus mean that this is regarded as a feedback interconnection of two passive systems. Accordingly, we can prove the following result.

Theorem 1 Consider the system interconnecting (16) with $\hat{\lambda}^0(0) \geq 0$ and the building dynamics (17)–(19) and (23) $\hat{\lambda}^b \geq 0$ for all $b = 1, 2, \ldots, N$ via $v_{\rm u} = y_{\rm b}$ and $v_{\rm b} = y_{\rm u}$. Suppose now that $w_{\rm a}^b \equiv d_{\rm a}^b$ and $w_{\rm q}^b \equiv d_{\rm q}^b$ for all $b = 1, 2, \ldots, N$. Then, if Assumptions 1 and 2 hold, $x_1^b \to z_{x1}^{b*}$ for all $b = 1, 2, \ldots, N$.

The above results are obtained assuming that both of $w_{\rm q}^b$ and $w_{\rm a}^b$ are constant. Since the ambient temperature is in general slowly varying, assuming a constant $w_{\rm a}^b$ looks reasonable. However, the heat gain $w_{\rm q}^b$ may contain high frequency components. To address the issue, we decompose the signal $w_{\rm q}^b$ into the DC components $d_{\rm q}^b$ and others $\tilde{w}_{\rm q}^b$ as $w_{\rm q}^b = d_{\rm q}^b + \tilde{w}_{\rm q}^b$. Then, a trivial extension of the well-known passivity theorem [10], [21] proves the following result.

Corollary 1 Suppose that $w_{\rm a}^b \equiv d_{\rm a}^b$ and $w_{\rm q}^b = d_{\rm q}^b + \tilde{w}_{\rm q}^b$ for all $b = 1, 2, \ldots, N$. Then, if Assumptions 1 and 2 hold, the system in Theorem 1 from the collection of $\tilde{w}_{\rm q}^b$ for all b to the collection of $x_1^b - z_{x1}^{b*}$ for all b has a finite $\mathcal{L}_2$ gain.

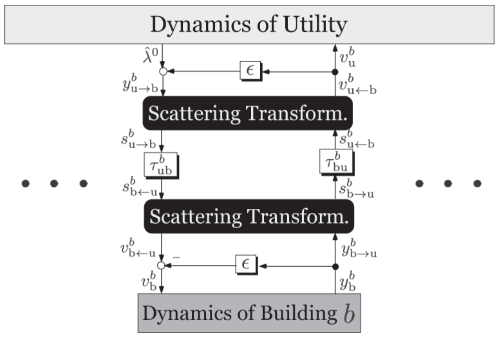

Fig. 5. Distributed algorithm with robustness against time delays.

V. Robust Algorithm against Time Delays

When implementing the distributed algorithm in Section III in real systems, time delays due to communication conditions exist and such delays can cause system instability. The goal of this section is to present a robust algorithm against delays. The communication between middle and low-level algorithms must suffer from delays but it can be expected to be short since the interaction is closed within a building. We thus focus on the delays between the high-level and the other two level algorithms, in other words, between utility and buildings. Hereafter, we denote the delays from the utility to building b as $\tau_{\rm ub}^b$ and delays in the opposite direction as $\tau_{\rm bu}^b$, which are both assumed to be unknown but constant.

In this section, we employ two additional assumptions.

Assumption 3 The functions $\bar{f}^1, \ldots, \bar{f}^N$ are linear functions, i.e., $\bar{f}^b(z_u^b) = (\psi^b)^\top z_u^b$ for some $\psi^b \in \mathbb{R}^{n_1^b}$.

Although a standard fan power model [5], [16] does not satisfy this assumption, it is in general much smaller than the cooling/heating power, and hence ignorable at least in the global specification (3d). Regarding the cooling/heating power, if we take the power consumption model in [22], this assumption is satisfied [2].

Assumption 4 The functions $f^1, \ldots, f^N$ are strongly convex, i.e., $\exists \rho > 0$ s.t. $(z - z')^\top(\nabla f^b(z) - \nabla f^b(z')) \geq \rho\|z - z'\|^2$ for any $z, z' \in \mathbb{R}^{n_1^b}$ for all $b = 1, 2, \ldots, N$.

This assumption is satisfied if we take the relaxation for the fan power consumption model in [16].

Let us now denote the signal that the utility receives from and sends to building b by $v_{\rm u\leftarrow b}^b$ and $y_{\rm u\to b}^b$ respectively. Similarly, the signals that the building receives from and sends to the utility by $v_{\rm b\leftarrow u}^b$ and $y_{\rm b\to u}^b$ respectively. Then, we choose $y_{\rm u\to b}^b$ and $y_{\rm b\to u}^b$ as follows.

$$y_{\rm u\to b}^b = \hat{\lambda}^0 + \epsilon v_{\rm u\leftarrow b}^b,\ y_{\rm b\to u}^b = y_{\rm b}^b = (\psi^b)^\top \hat{z}_u^b \tag{27}$$

with $\epsilon > 0$ such that $\epsilon\|\psi^b\|^2 < \rho\ \forall b$. The input $v_{\rm u}^b$ in (16) and the input $v_{\rm b}^b$ to the building dynamics are selected as

$$v_{\rm u}^b = v_{\rm u\leftarrow b}^b,\ v_{\rm b}^b = v_{\rm b\leftarrow u}^b - \epsilon y_{\rm b}^b, \tag{28}$$

[2]Precisely speaking, ψ^b depends on the ambient temperature in the model of [22], but this does not affect the subsequent discussions since it is assumed to be constant. This is why we skip the dependence for simplicity.

These operations are illustrated in Fig. 5.

Passivity of building dynamics in Lemma 4 and the utility in Lemma 5 is shown to be preserved w.r.t. the above input-output transformation under Assumptions 3 and 4 as below.

Lemma 6 Suppose $w_{\rm a}^b \equiv d_{\rm a}^b$ and $w_{\rm q}^b \equiv d_{\rm q}^b$. Then, under Assumptions 1–4, the system in Lemma 4 with $\hat{\lambda}^b(0) \geq 0$, (27) and (28) is passive from $-\tilde{v}_{\rm b\leftarrow u}^b$ to $\tilde{y}_{\rm b\to u}^b := \tilde{y}_{\rm b}^b$ for all $b = 1, 2, \ldots, N$, where $\tilde{v}_{\rm b\leftarrow u}^b := v_{\rm b\leftarrow u}^b - v_{\rm b\leftarrow u}^{b*}$ and

$$v_{\rm b\leftarrow u}^{b*} := v_{\rm b}^{b*} + \epsilon y_{\rm b}^{b*} = \lambda^{0*} + \epsilon(\psi^b)^\top z_u^{b*}.$$

Lemma 7 Under Assumption 1, the system (16) with $\hat{\lambda}^0(0) \geq 0$, (27) and (28) is passive from $\tilde{v}_{\rm u\leftarrow b} := [\tilde{v}_{\rm u\leftarrow b}^1\ \cdots\ \tilde{v}_{\rm u\leftarrow b}^N]^\top$ to $\tilde{y}_{\rm u\to b} := [\tilde{y}_{\rm u\to b}^1\ \cdots\ \tilde{y}_{\rm u\to b}^N]^\top$, where $\tilde{v}_{\rm u\leftarrow b}^b := v_{\rm u\leftarrow b}^b - v_{\rm u\leftarrow b}^{b*}$, $\tilde{y}_{\rm u\to b}^b := y_{\rm u\to b}^b - y_{\rm u\to b}^{b*}$,

$$v_{\rm u\leftarrow b}^{b*} := (\psi^b)^\top z_u^{b*},\ y_{\rm u\to b}^{b*} := \lambda^{0*} + \epsilon(\psi^b)^\top z_u^{b*}. \tag{29}$$

We next passify the communication block using so-called scattering transformation [10] as follows.

$$s_{\rm u\to b}^b = \frac{1}{\sqrt{2}}(y_{\rm u\to b}^b - v_{\rm u\to b}^b), s_{\rm u\leftarrow b}^b = \frac{1}{\sqrt{2}}(y_{\rm u\leftarrow b}^b + v_{\rm u\leftarrow b}^b), \tag{30a}$$

$$s_{\rm b\leftarrow u}^b = \frac{1}{\sqrt{2}}(v_{\rm b\leftarrow u}^b - y_{\rm b\leftarrow u}^b), s_{\rm b\to u}^b = \frac{1}{\sqrt{2}}(v_{\rm b\to u}^b + y_{\rm b\to u}^b). \tag{30b}$$

for all $b = 1, 2, \ldots, N$. The utility (building b) sends $s_{\rm u\to b}^b$ ($s_{\rm b\to u}^b$) to every building b (utility). The signal $s_{\rm u\to b}^b$ ($s_{\rm b\to u}^b$) is received by building b (utility) as $s_{\rm b\leftarrow u}^b$ ($s_{\rm u\leftarrow b}^b$) after the delay $\tau_{\rm ub}^b$ ($\tau_{\rm bu}^b$), namely the following equations hold.

$$s_{\rm b\leftarrow u}^b(t) = s_{\rm u\to b}^b(t - \tau_{\rm ub}^b),\ s_{\rm u\leftarrow b}^b(t) = s_{\rm b\to u}^b(t - \tau_{\rm bu}^b). \tag{31}$$

The utility and building b then compute their inputs $v_{\rm u}^b$ and $v_{\rm b}^b$ from (30) and (28). For simplicity, we also assume that $s_{\rm u\leftarrow b}^b(t) = 0$ and $s_{\rm b\leftarrow u}^b(t) = 0$ for any $t < 0$ and for all b.

Then, we have the following lemma.

Lemma 8 The scattering transformation (30) with (31) is passive from $[-\tilde{y}_{\rm u\to b}^b\ \tilde{y}_{\rm b\to u}^b]^\top$ to $[\tilde{v}_{\rm u\leftarrow b}^b\ \tilde{v}_{\rm b\leftarrow u}^b]^\top$.

We are now ready to prove the main result of this section.

Theorem 2 Consider the system (16)–(19) with (23), (27), (28), and the communication block (30) and (31) for all $b = 1, 2, \ldots, N$. Suppose that $\hat{\lambda}^0(0) \geq 0$, $\hat{\lambda}^b(0) \geq 0$, $w_{\rm a}^b \equiv d_{\rm a}^b$ and $w_{\rm q}^b \equiv d_{\rm q}^b$ for all $b = 1, 2, \ldots, N$. Then, under Assumptions 1–4, $x_1^b \to z_{x1}^{b*}$ holds for all $b = 1, 2, \ldots, N$.

VI. Simulation

We finally demonstrate the present algorithm through simulation, where we prepare 10 of the same building and the same profile of the ambient temperature data as [7]. The heat gains in each building are generated by random linear combinations of the data in [7]. The cost functions and constraints are also the same as [7] but we only add a global constraint (3d) with $\gamma = 12.7$. Other parameters and gains are set to the same value of [7].

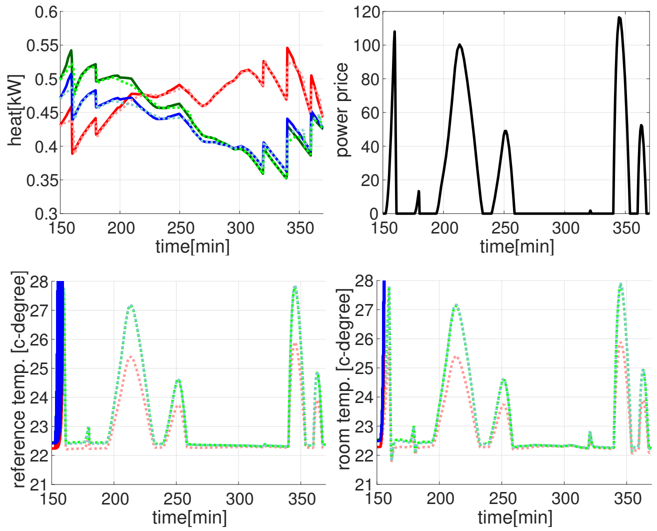

Fig. 6. Time responses of key variables of building 2 for the algorithm in Section III.

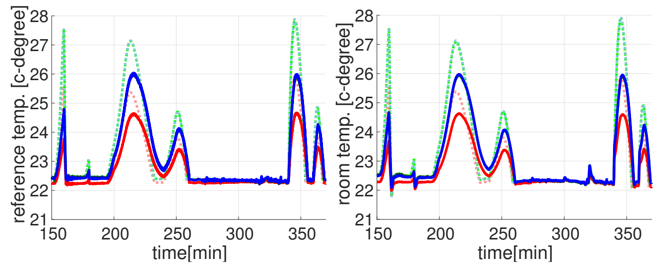

Fig. 7. Time responses for the robust algorithm in Section V.

Let us first apply the algorithm in Section III. Then, the resulting system trajectories associated with building 2 are illustrated in Fig. 6 by the dotted curves with light colors. The top-left figure shows the trajectories of the estimated heat gains, where the solid curves are the actual heat gains. It is confirmed that the disturbance is almost correctly estimated. The top-right figure illustrates the trajectory of the power price $\hat{\lambda}^0$. During the period with positive $\hat{\lambda}^0$, the constraint (3d) gets active and the buildings reduce the power consumption at the cost of the human comfort as shown in the bottom figures, where the left describes the estimated optimal zone temperatures and the right shows the actual ones. In these figures, the solid curves are trajectories generated by the algorithm in Section III when we add delays $T^b_{\rm ub} = T^b_{\rm bu} = 2$s for all b. We see that the system is destabilized by the delays.

We thus apply the robust algorithm presented in Section V with $\epsilon = 0.5$, and then we have the trajectories depicted by solid curves in Fig. 7. It is seen that the system stability is maintained in the presence of delays, although the response speed to the violation of (3d) is deaccelerated. Improving the speed is left as a future work of this paper.

VII. Conclusion

In this paper, we presented a novel hierarchical/distributed optimization algorithm for HVAC optimization and control in multiple buildings. The presented solution was designed based on the primal-dual algorithm and passivity-based physics-optimization interconnection presented in [7]. We then proved convergence of the zone temperatures to the optimal ones based on passivity. The algorithm was further extended so as to ensure robustness against inter-layer time delays using the scattering transformation.

References

[1] A. Afram, F. Janabi-Sharif, "Theory and applications of HVAC control systems : A review of model predictive control (MPC)," *Building and Environment*, vol. 72, pp. 343–355, 2014.

[2] F. Oldewurtel, A. Parisio, C.N. Jones, D. Gyalistras, M. Gwerder, V. Stauch, B. Lehmann and M. Morari, "Use of model predictive control and weather forecasts for energy efficient building climate control," *Energy and Buildings*, vol. 45, pp. 15–27, 2012.

[3] A. Aswani, N. Master, J. Taneja, D. Culler and C. Tomlin, "Reducing transient and steady state electricity consumption in HVAC using learning-based model-predictive control," *Proc. IEEE*, vol. 100, no. 1, pp. 240–253, 2012.

[4] Y. Ma, A. Kelman, A. Daly and F. Borrelli, "Predictive control for energy efficient buildings with thermal storage: modeling, stimulation, and experiments," *IEEE Control Syst.* vol. 32, no. 1, pp. 44–64, 2012.

[5] Y. Ma, J. Matusko and F. Borrelli, "Stochastic model predictive control for building HVAC systems: Complexity and conservatism," *IEEE Trans. Control Sys. Tech.*, vol. 23, no. 1, pp. 101–116, 2015.

[6] S. Goyal, H. Ingley and P. Barooah, "Zone-level control algorithms based on occupancy information for energy efficient buildings," *Proc. American Control Conference*, pp. 3063–3068, 2012.

[7] T. Hatanaka, X. Zhang, W. Shi, M. Zhu, and N. Li "An Integrated Design of Optimization and Physical Dynamics for Energy Efficient Buildings: A Passivity Approach," Proc. 1st IEEE Conference on Control Technology and Applications, to be presented, 2017.

[8] A. Cherukuri, E. Mallada, and J. Cortés, "Asymptotic convergence of constrained primal-dual dynamics," *System and Control Letters*, vol. 87, pp. 10–15, 2016.

[9] S. Boyd and L. Vandenberghe, *Convex Optimization*, Cambridge University Press, 2004.

[10] T. Hatanaka, N. Chopra, M. Fujita and M.W. Spong, *Passivity-Based Control and Estimation in Networked Robotics*, Communications and Control Engineering Series, Springer-Verlag, 2015.

[11] C. Zhao, U. Topcu, N. Li and S. Low "Design and stability of load-side primary frequency control in power systems," *IEEE Trans. Automatic Control*, vol. 59, no. 5, pp. 1177–1189, 2014.

[12] E. Mallada, C. Zhao and S. Low, "Optimal load-side control for frequency regulation in smart grids," *Proc. 52nd Annual Allerton Conf. Communication, Control, and Computing*, pp. 731–738, 2014.

[13] N. Li, L. Chen, C. Zhao and S.H. Low "Connecting automatic generation control and economic dispatch from an optimization view," *IEEE Trans. Control of Network Sys.*, vol. 3, no. 3, pp. 254–264, 2015.

[14] X. Zhang, A. Papachristodoulou and N. Li, "Distributed optimal steady-state control using reverse- and forward-engineering," *Proc. 54th IEEE Conf. Decision and Control*, pp. 5257–5264, 2015.

[15] T. Stegink, C.D. Persis and A. van de Shaft, "A unifying energy-based approach to optimal frequency and market regulation in power grids," arXiv:1510.05420v1, 2015 (downloadable at `https://arxiv.org/abs/1510.05420v1`).

[16] X. Zhang, W. Shi, X. Li, B. Yan, A. Malkawi and N. Li, "Decentralized and distributed temperature control via HVAC systems in energy efficient buildings," *Automatica*, submitted, 2016.

[17] J.T. Wen, S. Mishra S. Mukherjee, N. Tantisujjatham and N. Minakais, "Building Temperature Control with Adaptive Feedforward," *Proc. 52nd IEEE Conf. Decision and Control*, pp. 4827–4832, 2013.

[18] A. Agarwal and J.C. Duchi "Distributed delayed stochastic optimization," *Proc. 51st IEEE Conf. Dec. and Control*, pp. 5451–5452, 2012.

[19] T. Hatanaka, N. Chopra, T. Ishizaki and N. Li, "Passivity-Based Distributed Optimization with Communication Delays Using PI Consensus Algorithm," arXiv:1609.04666, 2016.

[20] M. T Hale, A. Nedić and M. Egerstedt, "Cloud-based centralized/decentralized multi-agent optimization with communication delays," Proc. 54th IEEE Conf. Dec. and Control, pp. 700–705, 2015.

[21] A.J. van der Schaft, *L2-Gain and Passivity Techniques in Nonlinear Control,* 2nd ed. Com. and Contr. Eng. Series. Springer, London, 2000.

[22] M. Maasoumya, M. Razmara, M. Shahbakhti, and A.S. Vincentelli, "Handling model uncertainty in model predictive control for energy efficient buildings," Energy and Buildings, vol. 77, pp. 377–392, 2014.